Digest Journal of Nanomaterials and Biostructures Vol. 10, No. 4, October - December 2015, p. 1329 - 1341

SYNTHESIS, CHARACTERIZATION AND TESTING OF MCM-41/TiO_2 CATALYST FOR ORGANIC DYE DEGRADATION

M. SÖNMEZ[a,b*], D. GUDOVAN[a], R. TRUŞCA[a], A. FICAI[a], D. FICAI[a], E. ANDRONESCU[a], B. S. VASILE[a]
[a]*POLITEHNICA University of Bucharest, Faculty of Applied Chemistry and Material Science; 1-7 Polizu St., Bucharest, Romania;*
[b]*National Research & Development Institute for Textiles and Leather– Division: Leather and Footwear Research Institute, 93 Ion Minulescu St., Bucharest, Romania*

This work focused on obtaining the MCM-41 substrate material and MCM-41 photocatalyst loaded with varying percentages of TiO_2 (1 and 10%). Titanium dioxide precursor represented by titanium isopropoxide was introduced in mesoporous silica pores under vacuum, followed by hydrolysis. Synthesized powders were morphologically characterized by (SEM and HRTEM) and compositionally by (FTIR, EDAX, elemental analysis, XRD). The obtained results confirm the synthesis of MCM-41 mesoporous silica with hexagonal pores loaded with TiO_2 nanoparticles. Synthesized powders were subsequently used in studies of azoic dye (tartrazine) adsorption/removal from aqueous solutions. Adsorption studies were carried out on a UV-VIS spectrophotometer at 427 nm. The determinations were carried out by contacting an amount of ~0.100g of MCM-41 powders, uncalcined MCM-41, MCM-41/1%TiO_2, and MCM-41/10%TiO_2 with 25 ml of tartrazine solution with constant concentration of 5 mg/L. The influence of contact time (0 to 216h) and the ability of synthesized powders to remove tartrazine were monitored. The degree of decolourisation after a 216h contact time with tartrazine solution varies as follows: MCM-41/10%TiO_2 (100%) > MCM-41/1%TiO_2 (99.88%) > uncalcined MCM-41 (99.12%) > MCM-41 calcined at 550°C (17.64%).

(Received September 30, 2015; Accepted November 23, 2015)

Keywords: Mesoporous silica, Anatase, Organic azoic dyes, Photocatalytic activity, Tartrazine

1. Introduction

Tartrazine is an azoic dye, also known as FD&C Yellow No.5, often used as dye in the pharmaceutical, food and cosmetics industries [1]. The use of tartrazine in the pharmaceutical industry, as dye in the composition of various drugs (like vitamins, antacids, medicinal capsules, etc.), was approved by the FDA (*Food and Drug Administration*) [2;3], for both internal and external use, as well as around the eyes. Tartrazine is, however, considered an extremely toxic material for humans and may cause allergic reactions (including bronchial asthma) among hypersensitive persons. Tartrazine is often associated with allergies and hypersensitivity reactions, particularly in patients with asthma or aspirin intolerance. Tartrazine hypersensitivity reactions include headaches, asthma attacks, itching or hives, insomnia, thyroid cancer and lupus. Due to tartrazine's high water solubility, its harmful effects are intensified.

Lately, special attention was paid to removing toxic organic dyes from the food and pharmaceutical industries to minimize devastating effects on the environment. Methods of removing toxic organic dyes include: adsorption, coagulation/flocculation, photo-catalytic decomposition, ozonation, microbial decomposition, wet air oxidation, sonochemical and electrochemical methods [4].

---

[*] Corresponding author: ficaimaria@yahoo.com

Photocatalytic degradation and mineralization of organic and inorganic pollutants by means of semiconductor TiO_2 have been extensively studied in order to solve environmental problems relating to waste waters and polluted air [5]. Among various metal oxide semiconductors, TiO_2 has been in the focus of photo-catalysis under UV irradiation because of its physical and chemical stability, insolubility, low cost, ease of availability, non –toxicity, electronic and optical properties and suitable band gap energy for photo-induced redox reactions [6;7]. However, the use of pure TiO_2 powders also has many disadvantages, such as: low quantum efficiency, small specific surface area and low adsorption ability, which significantly limit the efficiency of photo-catalysis [8;9]. These disadvantages limit the continuous flow use of TiO_2 powder at industrial scale, in part due to its high cost and difficult separation from the reaction medium [8]. Another limitation of using pure TiO_2 particles is related to low thermal stability, confirmed by the complete destruction of pores as a result of calcination. Heating to temperatures $> 450^0$C leads to phase transition, namely turning anatase into rutile [10]. Phase transition is associated with crystal size increase and decrease of specific area. Due to these disadvantages, many methods for TiO_2 deposition on mesoporous silica substrates were developed. Synthesis methods include titanium impregnation/grafting [11], titanium incorporation in mesoporous silica network, incorporation of preformed titania nanoparticles, sol-gel synthesis [12;6;13], co-hydrolysis and/or co-condensation, inner-pore hydrolysis/non-hydrolysis [14] and sol-gel/hydrothermal methods [15].

Lately, porous silicate materials such as clay, diatomite, activated carbon, zeolite [16] and mesoporous silica [17;18], have been intensely studied as ideal substrates for immobilization of TiO_2 nanopowders due to their special physicochemical properties such as high adsorption capacity. Special attention must be paid to the nature of the substrate, as it may also influence, to a great extent, photocatalytic activity, crystallinity of TiO_2 photocatalyst as well as adsorption of organic layers. An appropriate substrate promotes not only catalytic reactions by offering more active sites, but also enables recycling and reuse of the catalyst.

The advantages of using mesoporous silica as substrate in designing and functionalizing photocatalytic systems are the following [19]:

- high specific surface area and tunable pore sizes (2-50 nm);
- excellent transparency in a broad range of wavelengths – UV/VIS;
- mesoporous silica substrate with amorphous structure has many silanol groups able to support subsequent or post-synthesis changes;
- fine connectivity of the pores facilitating the transfer of organic substrates.

Direct synthesis such as co-condensation or pre-functionalization and post-synthesis are two methods for obtaining titania coated mesoporous silica materials. Direct synthesis is a relatively easy method of introducing titanium precursors on silica framework surfaces, but loading by titanium species is always low. Post-synthesis can induce a higher loading of titanium species on silica framework surfaces, but it is a complicated route, as the synthesis must be performed in the absence of water and oxygen. Also, post-synthesis generates other disadvantages such as destruction of the uniform mesostructure, as titanium species tend to form in channels or on the external surface of silica, with a negative impact on catalytic performance [20]. For applications such as heterogeneous catalysis or photocatalysis, Ti atoms have been incorporated into the silica framework, either by an ion implantation method, or by grafting of an organometallic complex on the surface [21]. More recently, a mesoporous titanosilicate (Ti-HMS) was prepared directly by the incorporation of Ti atoms into the MCM-41 framework [22]. Template titanium tetrabutoxide displacement has also been used. Shrinkage of the pore diameter is generally observed for high Ti loading. A mixed xerogel of composition $(TiO_2)_x$-$(SiO_2)_{1-x}$ has been prepared by the hydrolysis of tetraethyl orthosilicate in the presence of titanium isopropoxide.

Iglesias et al. [23] synthesized Ti-MCM-41 materials by co-condensation of tetraethylorthosilicate with two different titanium sources: titanocene dichloride (Cp_2TiCl_2) and titanium isopropoxide ($Ti(OiPr)_4$) – at room temperature. Ti-MCM-41 materials have been tested in the epoxydation of 1-octene and in the oxidative bromination of phenol red.

Mazinani et al. [24] synthesize TiO_2–SiO_2 mesoporous materials, by deposition of TiO_2 nanoparticles prepared by the sol–gel method onto the internal pore surface of wormhole-like mesoporous silica, by changing the hydrothermal temperature (70, 100, or 130 ^{0}C) and test photocatalytic properties for degradation of methylene blue in aqueous solution under UV light irradiation. As a result, efficient adsorption of organic pollutants onto porous substrates and/or the surface of TiO_2 nanoparticles is strongly dependent on the surface properties, such as hydrophilicity/hydrophobicity or surface change. Many other factors drastically influence active phase dispersion, such as: substrate nature, development method, calcination conditions, precursors and active phase loading. Thus, the use of an appropriate mesoporous substrate would contribute to obtaining better dispersed and stable metal particles, high specific surface and abundant pores leading to continuous improvement of catalytic performance [25].

This paper presents the synthesis and characterization of the mesoporous material based on MCM- 41 and loaded with 1 and 10% of TiO_2 and their testing as potential material with catalytic activity for degradation of tartrazine, a representative organic colorant. This study will be also applied in order to load MCM-based materials with different drugs or other biologically active components these systems being efficient drug delivery systems.

2. Materials and methods

2.1. Materials

All chemicals used in this study were of analytical grade. (CTAB) template - MW: 364.45 g/mol, assay ≥99%, mp: 248-251^{0}C, tetraethylortosilicate (TEOS) - MW: 208.33, bp: 163-1670C, d20: 0.933, ammonium hydroxide solution - 25% NH_3, titanium (IV) isopropoxide ($Ti[OCH(CH_3)_2]_4$) - MW: 284.22, refractive index: n20/D 1.464, bp: 232^{0}C, mp:14-17^{0}C, density: 0.96 g/mL at 20^{0}C, Ethyl alcohol (CH_3CH_2OH) - MW: 46.07g/mol, vapour density: 1.59 (vs air), vapour pressure: 44.6 mmHg (20^{0}C), were purchased from Sigma Aldrich, China and USA.

Tartrazine (Fig. ***1***), trisodium-5-hydroxy-1-(4-sulfonatophenyl)-4-(4-sulfonatophenylazo)-*H*-pyrazole-3-carboxylate, is an azoic dye with molecular formula $C_{16}H_9N_4Na_3O_9S_2$, MW: 534.37, and was purchased from Fluka, Switzerland.

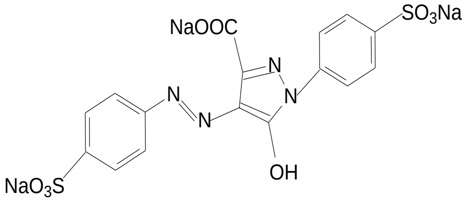

Fig. 1. Chemical structure of tartrazine

2.2. Substrate and photo-catalyst synthesis

2.2.1. MCM-41 substrate synthesis

MCM-41 mesoporous silica was synthesized using the methodology published by Melendez-Ortiz et al. [26]. Mesoporous silica with MCM-41 hexagonal pores is synthesized, using the following components and amounts: 0.5g of CTAB with the role of pore forming agent or template is magnetically stirred with 96ml distilled water at room temperature. For better homogenisation, the mixture was introduced into the ultrasound bath for approximately 15 minutes and maintained until the solution becomes completely clear. To this clear solution, 34ml ethanol and ammonia solution with a concentration of 25% are added under continuous mechanical stirring. After homogenization, 2.5ml of TEOS (tetraethylorthosilicate) was quickly injected in the form of fine drops and magnetically stirred for 3h, subsequently followed by filtration and drying. The surfactant is removed by calcination at 550^{0}C for 9 h, according to the DTA-TG analysis. The resulting powder was characterized by XRD, FTIR, SEM and TEM, confirming the formation of MCM-41 mesoporous silica with hexagonal pore structure.

2.2.2. MCM-41/TiO$_2$ photocatalyst synthesis

MCM-41/TiO$_2$ photocatalyst was synthesized using post-synthesis method. The titanium precursor was incorporated in the pores of mesoporous silica using an adequate amount of titanium (IV) isopropoxide (36μl and 360μl) reported to the amount of MCM-41 – 1g used, so that the final content of TiO$_2$ to became 1 and 10% respectively. The titanium precursor was absorbed into the mesopores under vacuum followed by hydrolysis of the precursors. In order to prevent hydrolysis and facilitate adsorption of titanium (IV) isopropoxide in the pores of mesoporous silica, the former is added as mixture in 10ml ethanol, followed by water addition and solvent evaporation in the oven at the temperature of 80^{0}C. The water was added in order to assure the hydrolysis of TiO$_2$ precursor, in high excess comparatively with the stoichiometric ratio (1mL, regardless the sample). The role of ethanol and the applied vacuum is to ensure the homogeneous distribution of the TiO$_2$ precursor inside the MCM-41 pores.

2.3. Characterization of MCM-41 and MCM-41/TiO$_2$ powders

The resulting MCM-41 mesoporous silica and MCM-41-TiO$_2$ photocatalysts were analyzed by different techniques. X-ray diffraction (XRD) analysis was performed using a Shimadzu XRD 6000 diffractometer at room temperature, Cu-Kα radiation from a Cu X-ray tube (ran at 15mA and 30 kV) was used to identify the main crystalline phases present in the samples. Infrared spectroscopy analysis (FTIR) performed using a Thermo iN10 MX FTIR microscope operated in reflection mode, was carried out to study their structural features. The surface morphology of samples was examined by scanning electron microscopy (SEM). SEM images were recorded on a QUANTA INSPECT F electron microscope equipped with a field emission gun and an energy dispersive detector (EDS), on samples covered with silver. UV-VIS measurements were made using a Thermo Evolution 300 spectrometer operated in transmission mode over the range of 190-1100nm for UV-VIS spectral recording or in quant mode for evaluating the content of Tartrazine, in solution.

2.4. Adsorption studies

Experimental studies were carried out by adsorption on a UV-VIS spectrophotometer, for retention and removal of azoic dye tartrazine, on simple and various TiO$_2$ precursors-doped MCM 41 mesoporous silica powder. In this regard, a stock solution was prepared in deionised water at a concentration of 5 mg/L. Solutions for adsorption tests were prepared by diluting the stock, yielding standard solutions with the following concentrations: 2, 1, 0.5 and 0.1 mg/L. The stock solution was also used to determine the wavelength at which the dye absorption is maximal, namely 427nm as well as to draw the calibration curve. Kinetic experiments were carried out by contacting a quantity of ~0.1000g simple MCM-41 powder or MCM-41/TiO$_2$ with 25ml of the tartrazine solution, 5mg/L at room temperature. At different predetermined time intervals, 2.5 ml of solution were removed, filtered through a 0.45µm filter, and subjected to analysis at 427nm to determine the residual dye concentration, in solution.

After equilibrium, the final concentration (C_f) was determined and the percentage of the removal of dye was calculated using the following relationship:

$$\text{Degree of decolourisation (\%DD)} = C_0 - C_f / C_0 \times 100$$

where C_0 and C_f are the initial and final (at equilibrium) concentrations of dye (mg/L), respectively.

The elemental analyses were recorded on a Thermo Scientific Flash 2000 Elemental Analyser, in CHNS mode. The samples were previously put in contact with distilled water or tartrazine solution (as presented above), washed twice with water, under vacuum followed by vacuum drying, overnight.

3. Results and discussion

3.1. Characterization of the photo-catalysts

3.1.1. X-ray diffraction (XRD)

The X-ray diffraction pattern exhibits the characteristic interferences of MCM-41, confirming the formation of the hexagonal mesoporous network. No other interferences can be identified, so MCM-41 was obtained with high phase purity.

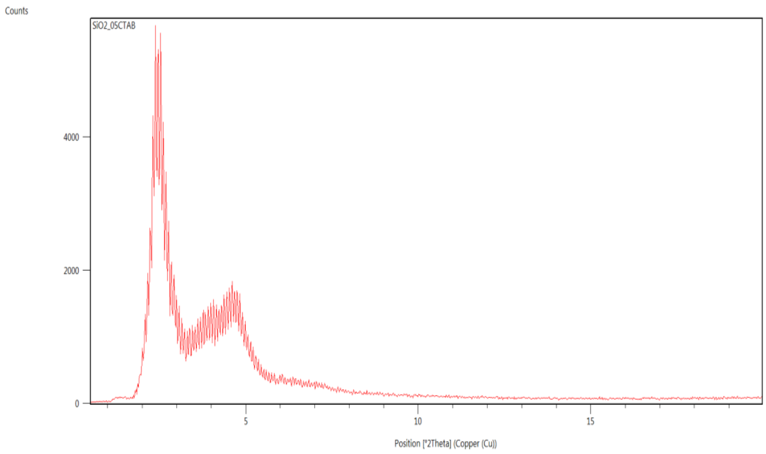

Fig. 2. X-ray diffraction recorded on the MCM-41 powder calcined at 550^{0}C

3.1.2. FTIR spectra of silica based photo-catalysts

FTIR data reveal the formation of the MCM-41 system based on the intense and characteristic peak from around 970 (Si-OH vibration), 1050 and 1240cm^{-1} (these two peaks can be assigned to the asymmetric stretching of Si-O-Si groups). The main peak of TiO_2 appears at ~400cm^{-1} but is overlapped over the bending vibration of Si-O-Si chain.

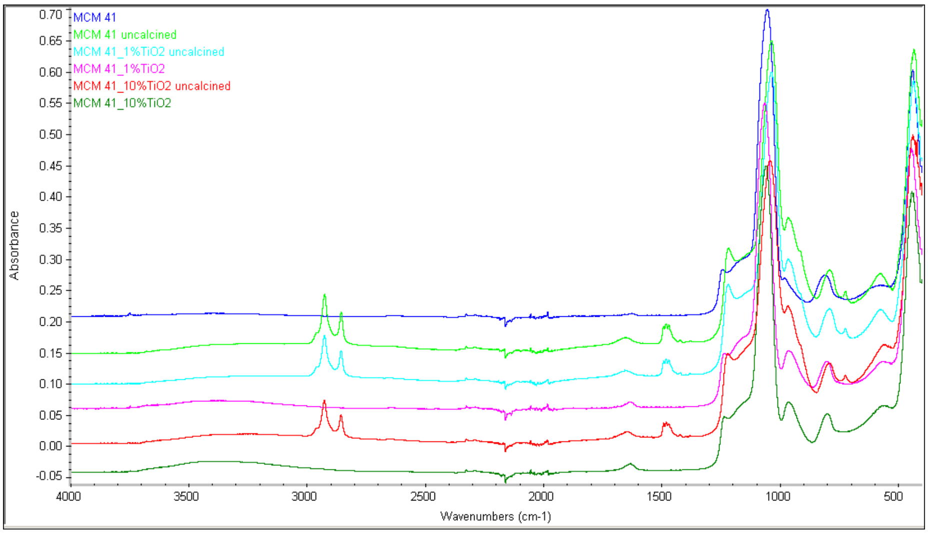

Fig. 3. FTIR spectra of synthesized powders

The calcination of the MCM-41 is done in order to remove the template agent. All the uncalcined samples present the peaks of the organic template (CTAB): especially the peaks from 2922, 2852, 1489, 1478, 1467cm^{-1}. Beside these peaks, there are also some peaks which are overlapped over the MCM-41 peaks and are hard to identify, even after deconvolution.

The peak from 1620-1650 as well as the broad peak from 3000-3500cm^{-1} can be associated with the vibrations of water molecules. It is worth mentioning that water is found in the three materials, even after their calcination, most probably due to the entrapment of water into the pores, the presence of TiO_2 favouring the absorption of water.

The calcination of the MCM-41 is done in order to remove the template agent. All the uncalcined samples present the peaks of the organic template (CTAB): especially the peaks from 2922, 2852, 1489, 1478, 1467cm^{-1}. Beside these peaks, there are also some peaks which are overlapped over the MCM-41 peaks and are hard to identify, even after deconvolution.

The peak from 1620-1650 as well as the broad peak from 3000-3500cm^{-1} can be associated with the vibrations of water molecules. It is worth mentioning that water is found in the three materials, even after their calcination, most probably due to the entrapment of water into the pores, the presence of TiO_2 favouring the absorption of water.

3.1.3. Scanning electron microscopy coupled with energy dispersive spectrometry

The morphology, size and particle size distribution of MCM-41, MCM-41/1%TiO_2 and MCM-41/10%TiO_2 powders were determined using SEM. SEM images of the powder calcined at 550°C are shown in Fig. 4A, B and C. The particles shape for the three types of powders are spherical, and sometimes distorted spherical shapes can be observed. It is also noticed that loading mesoporous silica with TiO_2 does not affect particle shape and no other particles can be identified on the surface of MCM-41. The particle size observed by SEM falls in the 200-500nm range, and basically do not depend on the content of TiO_2. This can be also explained by the fact that TiO_2 precursor is absorbed into the pores and consequently the TiO_2 nanoparticles are formed into these pores.

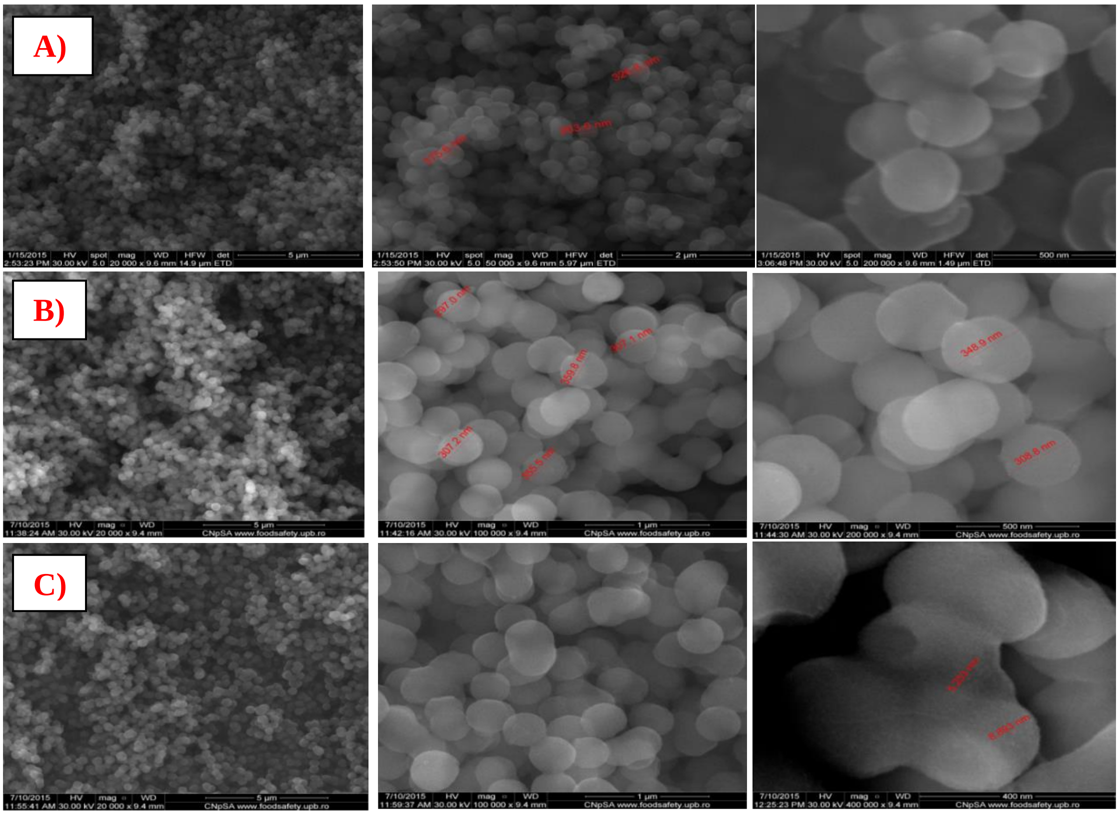

Fig. 4. SEM image of powders: MCM-41 (A), MCM-41/1%TiO_2 (B) and MCM-41/10%TiO_2 (C)

Fig. 5 presents the energy dispersive spectroscopic spectra of the two photocatalysts, namely MCM-41/1% TiO_2 and MCM-41/10% TiO_2. In both spectra the following elements can be identified: silicon, titanium, carbon and oxygen. Also, it can be seen that the relative intensity of the peaks corresponding to Ti increase in the case of MCM-41/10%TiO_2 comparing with the spectrum recorded on MCM-41/1%TiO_2. This indicates that, even if in SEM these particles are not visible they are present most probably inside the pores.

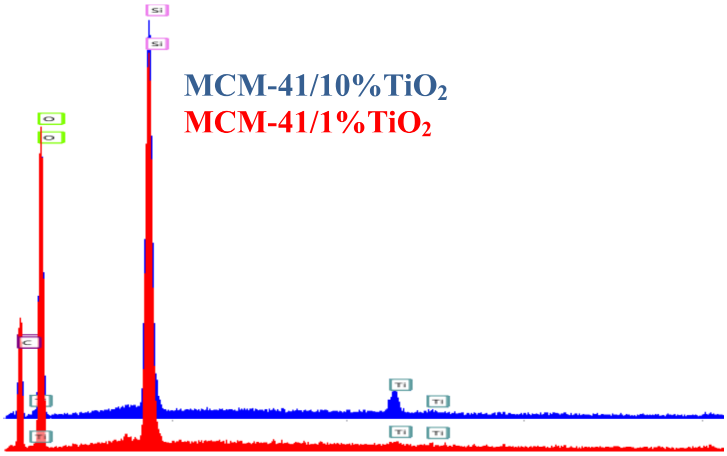

Fig. 5. EDAX spectra of MCM-41/1%TiO_2 and MCM-41/10%TiO_2

Table 1 presents the quantitative analysis performed on MCM-41/10%TiO_2 powder and confirm the presence of 9.95% of TiO_2, close to the expected value.

Table 1. Quantitative analysis of MCM-41/10%TiO_2 powder

Element	Weight content %	Atomic content %	Error %
O K	50.62	65.45	9.36
Si K	43.41	31.97	4.06
Ti K	5.97	2.58	6.15

3.1.4. Transmission Electron Microscopy

Fig. ***6*** and Fig. ***7*** present TEM images obtained for synthesized powders. For MCM-41 mesoporous silica (

Fig. ***6***), MCM-41/1%TiO_2 (Fig. ***7***, A) and MCM-41/10%TiO_2 photo-catalyst (Fig. ***7***, B), the mesoporous, ordered structure being highlighted at high resolution. Based on the high resolution TEM measurements, the presence of TiO_2 cannot be proved most probably because the TiO_2 nanoparticles are inside the pore structures of MCM-41.

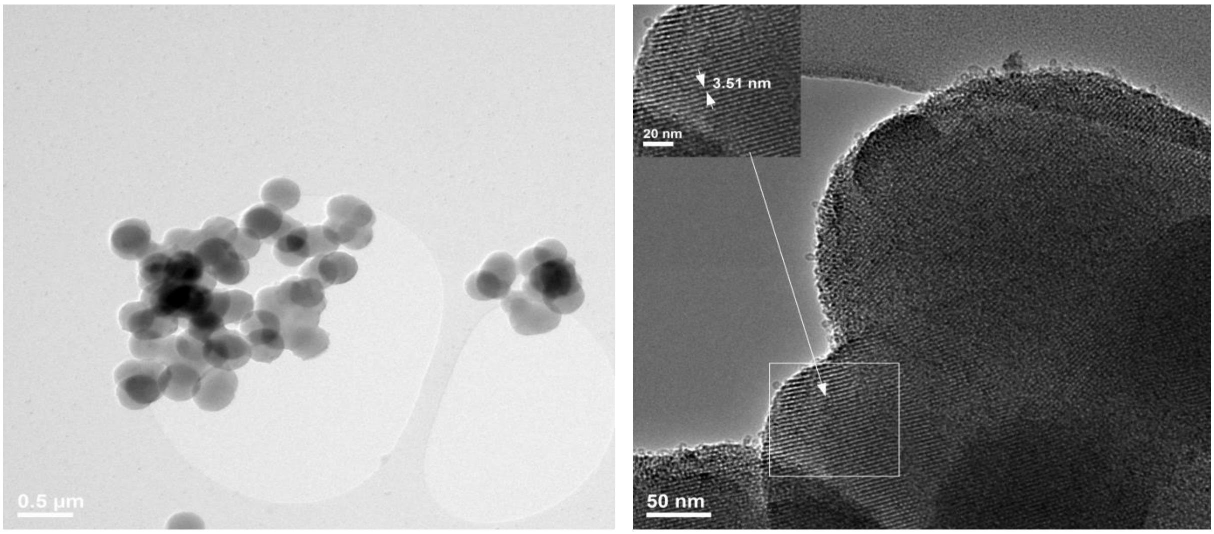

Fig. 6. Characteristic TEM images of MCM41

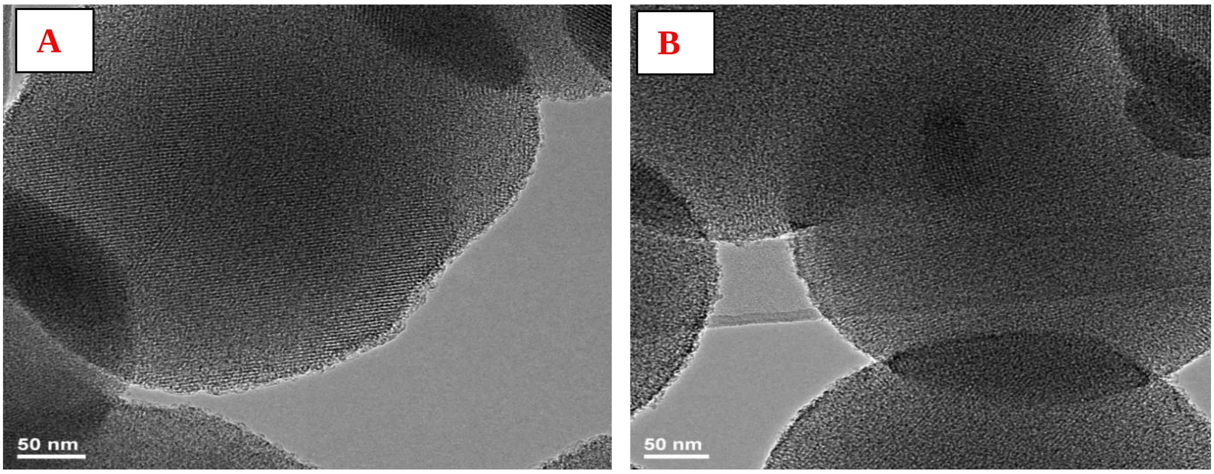

Fig. 7. TEM images of MCM-41/1%TiO_2 (A) and MCM-41/10%TiO_2 (B)

3.2. Adsorption tests carried out on synthesized powders for retention and removal of azo dye - tartrazine - and characterisation of powders after adsorption

We investigated the effect of contact time among the 4 types of previously synthesized powders: MCM-41, uncalcined MCM-41 and photocatalysts (MCM-41/1% TiO_2 and MCM-41/10% TiO_2) and the tartrazine solution with a constant concentration of 5mg/L at room temperature. Adsorption of the dye used, namely tartrazine, was investigated over time in the range of 0-216 hours.

3.2.1. Tartrazine removal tests

In Fig. ***8*** the Degree of decolorisation is plotted against the contact time. As Fig. ***8*** shows, the ability to remove tartrazine is significantly different depending on the type of powder used. When using calcined MCM-41 mesoporous silica we can see a weak affinity and consequently a low removal rate of only 17.64% after a contact time of 216 hours with tartrazine solution. It is very important to note that all determinations with the 4 types of powders were performed under the same conditions, using the same dye concentration, temperature and sampling time to minimize experimental errors. When using uncalcined MCM-41 sample, the removal capacity reaches ~100% even if the corresponding sample (MCM-41) does not reach 20% after 4 days. Uncalcined MCM-41 powder, probably due to the presence of template molecules into the pore favour the absorption of the dye into the pores assuring a better/reasonable degradation on the tartrazine, and ~88% after 120h. After a contact time of 216 hours with the solution of tartrazine, the percentage of dye removed is 99.12%.

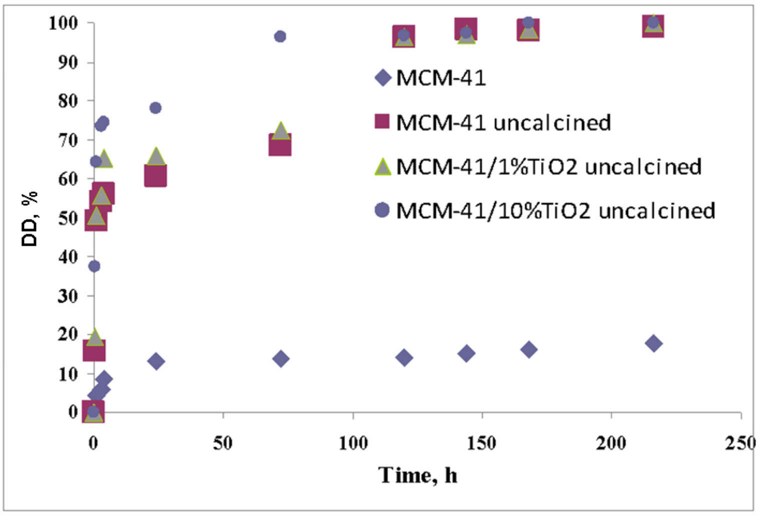

Fig. 8. Ability to remove tartrazine, MCM-41 and uncalcined MCM-41 powders and photo-catalysts (MCM-41/1%TiO_2 and MCM-41/10%TiO_2)

The two types of photocatalysts synthesized with various content of TiO_2 (1 and 10%), exhibit a much faster two dye photolysis speed. Thus, when using MCM-41/1%TiO_2 the dye decolouration is 38% within one hour, 86.83% in 120h and 93.18% in 216 h. The total percentage of tartrazine decolourised in 216h is 99.88%. When using MCM-41/10%TiO_2, the decolourisation rate is superior compared to all powders. Thus, for a contact time of 1h, the degree of decolourization is 64%, for 120h is 96.57% and for 216 it reaches ~100%.

3.2.2. Characterisation of the MCM-41 based materials after removal tests

The powders were characterised after the removal tests have been completed. The samples were analyzed by SEM, elemental analysis and FTIR.

Fig. 9 presents characteristic SEM image of the MCM-41/1%TiO_2 powder after 216 hours contact with tartrazine solution. As seen, the dye adsorption does not significantly affect the particles shape and size. Also, the surface of these materials does not change as a consequence of the tartrazine absorption. This can be easily seen taking as reference SEM images performed on MCM-41/1%TiO_2 powder, where the particle sizes were in the range of 297 - 359.8nm while after dye degradation study the particle size varies in the range of 291.8 and 350nm being in a very good agreement with the control sample. The very small differences are rather a consequence of the particle size heterogeneity instead of the absorption of tartrazine.

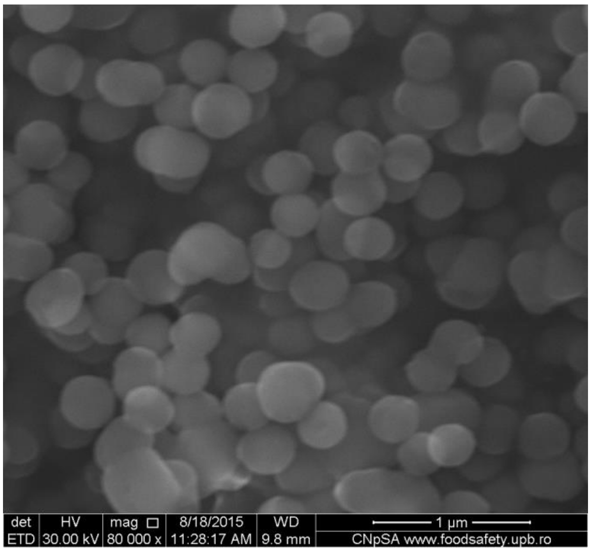

Fig. 9. SEM image MCM-41/1%TiO$_2$ photocatalyst after tartrazine absorption

FTIR was also used to identify the presence of the tartrazine after the tartrazine removal study (Figure 10). The spectrum of the MCM-41_uncalcined sample seems very similar with that of MCM-41_uncalcined/tartrazine obtained after contacting MCM-41_uncalcined sample with 5mg/L tartrazine solution, for 216h. The influence of the contacting tartrazine solution with uncalcined MCM-41 was analysed after the subtraction of the spectrum of uncalcined MCM-41 from the spectrum of MCM-41_uncalcined/tartrazine. The resulting spectrum is presented into the insert. It can be seen that some regions suffer some important changes, shifting or even disappearance of some bands. Based on a paper published by Gobara and Baraka, [27], the disappearance of the band from 1560 cm^{-1} is a proof of the degradation of N=N (azo) group which explain the mechanism of discoloring of the tartrazine solution via a degradation instead of an absorption mechanism, and based on the elemental analysis the degradation products leave the pores of the MCM-41 system.

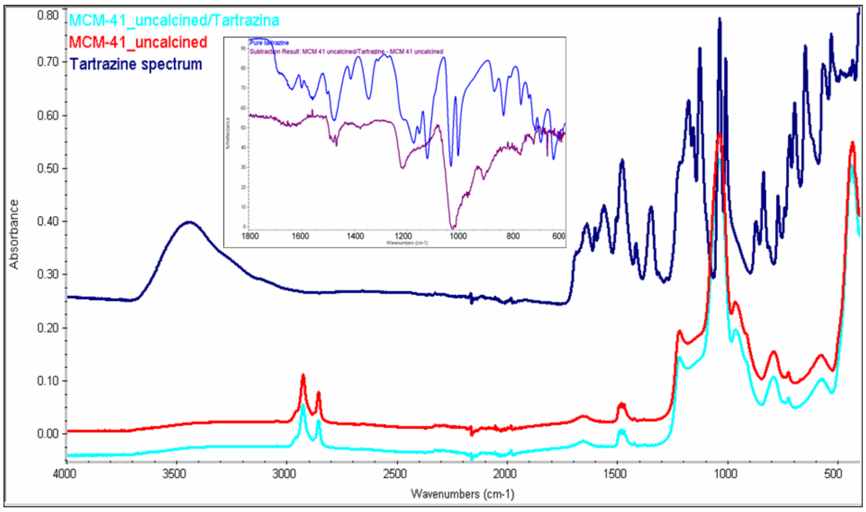

Fig. 10. FTIR spectra of pure tartrazine, MCM-41_uncalcined and MCM-41_uncalcined after 216h of contact with tartrazine solution; insert represent the result of the subtraction of the MCM-41_uncalcined from the MCM-41_uncalcined/tartrazine spectrum (magenta) compared with the tartrazine spectrum (blue); 600 – 1800 range

The elemental analyses (Table 2) were recorded on samples maintained for 216h in pure distilled water or in tartrazine solution followed by washing twice with water, filtered under vacuum and finally dried overnight at 50^{o}C, under vacuum. The results highlight that the carbon content of the uncalcined samples exhibit higher C and H content because of the presence of the templating agent (CTAB). Even if Tartrazine also contains N and S, these data present higher errors and are not presented in this study (N is 10.48% while S is 17.10% in pure trisodium tartrazine). Comparing the content of C for the four samples after maintaining them in water and tartrazine solution (denoted with /tartrazine no (marginal) differences appear between the samples maintained 216h in water or tartrazine which means that no (or only limited amount of) tartrazine is absorbed into the samples. The low hydrogen content of the MCM-41 (calcined at 550^{o}C) in both cases (after 216h of contact with water or tartrazine solution) reveals that water penetrates into the pores very slowly.

Table 2. Elemental analysis of the samples after immersing in water or tartrazine solution

Sample	Identified elements	
	C	**H**
MCM-41	6.3813	0.7884
MCM-41 uncalcined	34.4903	6.8612
MCM-41/1%TiO_2 uncalcined	32.3984	6.0759
MCM-41/10%TiO_2 uncalcined	32.5378	6.0579
MCM-41/tartrazine	6.3317	0.7499
MCM-41 uncalcined/tartrazine	34.4845	6.8752
MCM-41/1%TiO_2 uncalcined /tartrazine	32.4694	6.1623
MCM-41/10%TiO_2 uncalcined /tartrazine	32.3509	6.0882

4. Conclusions

This study was conducted in order to synthesize MCM-41 mesoporous silica (as substrate), its doping with TiO_2 particles and testing the ability of these powders to remove by photodissociation organic azo dyes (tartrazine being a common representative of this class) from synthetic aqueous solutions. The results obtained by XRD and (HR)TEM demonstrate that MCM-41 mesoporous silica with hexagonal pore structure was successfully obtained. Also, doping MCM-41 with TiO_2 particles using vacuum adsorption followed by hydrolysis was proved to be optimal to synthesize powders with photocatalytic properties. Ti peaks obtained by EDAX can be clearly visualized and with increasing amounts of isopropoxide, their intensity increases, which demonstrates that TiO_2 precipitation occurs even if no evidence can be made by TEM. TEM images confirm powders with highly ordered structure. Adsorption tests for tartrazine removal were carried out at 427 nm, monitoring the influence of contact time on the adsorption capacity of the powder. For adsorption tests the four types of powder were used, namely, MCM-41 (calcined), uncalcined MCM-41, MCM-41/1%TiO_2, and MCM-41/1%TiO_2. The time in which adsorption studies were carried out was between 0 and 216 hours. The results demonstrate that with increasing contact time of powders with the 5mg/L tartrazine solution the degree of discolouring/degradation also increases. Thus, the degree of discolouring/degradation (DD%) of tartrazine after a contact time of 216h varies as follows: MCM-41/10%TiO_2_uncalcined (100%)> MCM-41/1%TiO_2_uncalcined (99.88%) > MCM-41_uncalcined (99.12%) > MCM-41 calcined at 550°C (17.64%).

Therefore, one can conclude that the use of synthesized powders based on uncalcined MCM-41, MCM-41/1%TiO_2 and MCM-41/10%TiO_2 offers promising alternatives to remove toxic organic dyes from aqueous discharges solutions from the food and pharmaceutical industries. Also, due to high affinity for adsorption and removal of toxic dyes and due to non-toxicity of these powders, the areas of use can be extended to strictly pharmaceutical applications, namely, for synthetic tartrazine removal from various types of medicinal tablets. This would be possible by contacting the tablets with distilled water. Because of its high water solubility, tartrazine dissolves readily and can be degraded on synthesized mesoporous silica powders.

Further works will be done in order to apply this methodology of loading mesoporous substrates with drugs or other active components as well as to fully elucidate the mechanism of degradation. The use of different MCM-based support materials will be exploited to obtain and control the delivery rate of different active components.

Acknowledgements

The work has been funded by the Sectorial Operational Program Human Resources Development 2007-2013 of the Ministry of European Funds through the Financial Agreement POSDRU/159/1.5/S/134398. Some analyses using the R&D equipments acquired via an EU-funding grant POSCCE-A2-O2.2.1-2013-1/Priority axis 2, Project #638/12.03.2014, SMIS-CSNR code #48652.

References

[1] K.A. Amina, H. Abdel Hameid, A.H. Abd Elsttar,. Food and Chemical Toxicology. **48**(10), 2994 (2010).
[2] J.B. Hallagan, D.C. Allen, J.F. Borzelleca, Food and Chemical Toxicology. **33**(6), 515 (1995).
[3] S.C. Smolinoke, Handbook of food, drug and cosmetic excipients. CRC Press LLC, Florida. 1992
[4] S. Banerjee, M.C. Chattopadhyaya,. Arabian Journal of Chemistry. xx, 1 (2013).
[5] A.S. Mahmoud, A. Szegedi, A.K. Aboul Gheit, Chemistry and Materials Research. **6**(9), 16 (2014)
[6] D. Kannaiyan, S. T. Kochuveedu, Y.H. Jang, J.Y. Jang, Y.J. Lee, J. Lee,. Polymers. **2**, 490 (2010).
[7] B. Faure, G. Salazar-Alvarez, A. Ahniyaz, I. Villaluenga, I. Berriozaba, Y. R De Miguel, L. Bergstrom, Sci. Technol. Adv. Mater. **14**, 1 (2013).
[8] Z. Sun, C. Bai, S. Zheng, X. Yang, L.R. Frost,. Applied Catalysis A: General. **458**, 103 (2013)
[9] C.W. Kim, U. Pal, S. Park, H.Y. Kim, J. Kim, S.Y. Kang,. RSC. Adv., **2**, 11969 (2012).
[10] B. Elgh, N. Yuan, S.H. Cho, D. Mager, M. Philipp, S.V. Roth, K.B. Yoon, P. Müller-Buschbaum, O. Terasaki, A.E.C. Palmqvist, Apl. Mater. **2**, 1 (2014).
[11] M. Guidotti, C. Pirovano, N. Ravasio, B. Lázaro, J. M. Fraile, J.A. Mayoral, B. Coq, A. Galarneau, Royal Society of Chemistry. **11**, 1421 (2009).
[12] Y. Chunxiao, Y. Lanfang, T. Linlin, F. Xueling, Journal of Physics. **188**, 1 (2009).
[13] S. Ghodke, R. Patel, U. Chudasama, International Journal of Innovative Research in Science. **4**(1), 18735 (2015).
[14] J. Janlamool, B. Jongsomjit, Sci. J. UBU. **1**(2), 35 (2010).
[15] Y.C. Liu, Y.F. Lu, Y.Z. Zeng, C.H. Liao, J.C. Chung, T.Y. Wei,. International Journal of Photoenergy. **2011**, 1 (2011).
[16] F. Hossein, N. Shakiba, Iran. J. Chem. Chem. Eng. **32**(3), 9 (2013).
[17] A. Nishimura, Y. Yamano, T. Hisada, M. Hirota, E. Hu, International Journal of Photoenergy. **2010**, 1 (2010).
[18] E.D. Mihaiescu, D. Gudovan, E. Andronescu, U.P.B. Sci. Bull., Series B, **77**(2), 19 (2015).
[19] X. Qian, K. Fuku, Y. Kuwahara, T. Kamegawa, K. Mori, H. Yamashita,. Chem.Sus.Chem. **7**, 1528 (2014).
[20] Z. Wang, F. Zhang, Y. Yang, B. Xue, J. Cui, N. Guan, Chem.Mater. **19**(13), 3286 (2007).
[21] F. Leroux, P.J. Dewar, M. Intissar, G. Ouvrard, L. F. Nazar, J. Mater. Chem. **12**, 3245 (2002).
[22] S.H. Jang, M.J. Kim, J. R. Ko, W.S. Ahn, Bull. Korean Chem. Soc. **26**(8), 1214 (2005).
[23] J. Iglesias, J.A. Melero, M. Sánchez-Sánchez, Journal of Molecular Catalysis A: Chemical. **132**, 112 (2010).

[24] B. Mazinani, A. Beitollahi, A.K. Masrom, N. Yahya, T.S.Y. Choong, S.M. Ibrahim, J. Javadpour, Res. Chem. Intermed. **38**(8), 1733 (2012).
[25] H. Kolev, S. Todorova, A. Naydenov, R. Ene, G. Ivanov, V. Parvulescu, G. Kadinov, Athens Journal of Natural & Formal Sciences. **1**(1), 9 (2014).
[26] H.I. Melendez-Ortiz, L.A. Garcia-Cerda, Y. Olivares-Maldonado, J.A. Castruita, Ceramics International. **38**, 6353 (2012).
[27] M. Gobara, A. Baraka, international letters of chemistry, physics and astronomy, **14**(1), 106 (2014).